The Effect of Solar Radiation on the Ampacity of an Underground Cable with XLPE Insulation

Dardan Klimenta[1], Miroljub Jevtić[1], Jelena Klimenta[2], Bojan Perović[1]

[1]University of Priština in Kosovska Mitrovica, K. Mitrovica, Serbia, and [2]Independent Consultant in the Field of Urban and Spatial Planning, Niš, Serbia

Introduction

- The relevant standards [1-3] do not take into account the thermal effect of the Sun on the ampacity of underground power cables.
- The number of research papers dealing with this effect is small.
- All of these papers were written by Klimenta et al. [4-6].
- There are also researchers who found that solar radiation only affects the cables laid at law depths [7], and researchers who concluded that the effect of the Sun can not be ignored in the case of cables under dynamic loading [8-10].
- In this paper, the quantification of the thermal effect of the Sun on the cable ampacity was performed for different laying depths of the cable (0.4, 0.7 and 1 m), different surfaces of the pavement above the cable (cool white coating, acrylic white paint, uncoated concrete blocks, uncoated asphalt and acrylic black paint), different dimensions of the cable bedding (case I – the bedding of standard size, and case II – the trench completely filled with bedding material), various load currents, various solar irradiances and different operation conditions (the most unfavourable summer conditions and the most common winter conditions).
- The considered XP-00 4×16 mm² 0.6/1 kV cable has cross-linked polyethylene (XLPE) insulation and corresponds to the N2XY type.
- Simulation results were obtained using the finite-element method (FEM) in COMSOL and were compared with the corresponding experimental data from [4-6].

Experimental Background

- The apparatus, procedure, materials and measurement results that were used as an experimental background for this study are described in detail in [4-6]. In [4-6], the following experiments were conducted: (i) with pavement made of concrete blocks, (ii) with concrete-pavement coated with acrylic white paint, and (iii) with concrete-pavement coated with acrylic black paint.
- For the purposes of comparing the simulation results with the experimental data from [4-6], the following three points are singled out: A – on the outer surface of the physical model of the cable, B –on the lower surface of the pavement above the physical model of the cable, and C – on the upper surface of the pavement above the physical model of the cable.
- The temperature at point A was obtained by averaging the measured values at three different points along the physical model of the cable, while the temperatures at points B and C were measured directly.
- Points A, B, and C are marked within the small-size computational domain, which is used for FEM-based simulations in COMSOL.

2D FEM-Based Model

- A two-dimensional (2D) FEM-based heat conduction model is created based on the following equation [4]:

$$\frac{\partial}{\partial x}\left(k\frac{\partial T}{\partial x}\right)+\frac{\partial}{\partial y}\left(k\frac{\partial T}{\partial y}\right)+Q_v=0 \qquad (1)$$

where k is the thermal conductivity in W/(m·K); T is the temperature in K; x, y are Cartesian spatial coordinates in m; and Q_v is the volume power of heat sources in W/m³.

- The volume power of heat sources in the phase conductors is

$$Q_v=\frac{R_{ac}(T_{cp})}{S'_c}\cdot I^2 \qquad (2)$$

where $R_{ac}(T_{cp})$ is the a.c. resistance per unit length of a single copper conductor at temperature T_{cp}=90 °C, T_{cp} is the continuously permissible temperature of the XLPE-cable in °C, I is the cable load current in A, and S'_c is the geometric cross-section area in m².

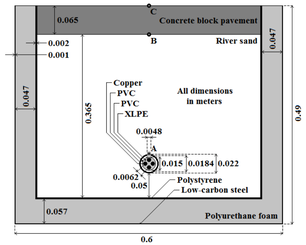

Figure 2. Presentation of the small-size computational domain corresponding to the experimental apparatus.

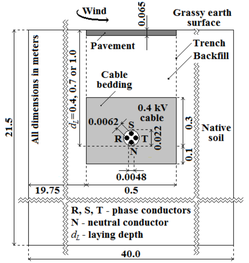

Figure 2. Presentation of the large-size computational domain.

TABLE I. DETAILS ON FINITE ELEMENT MESHES AND MESH INDEPENDENCE TESTS

Domain	Finite element mesh				Temp. differences
	Automatically generated		After refinement		
	No. of nodes	*No. of elements*	*No. of nodes*	*No. of elements*	°C
Small	15146	29101	59392	116404	<0.002
Large, with d_L=0.4 m	1776	3459	7010	13836	<0.03
Large, with d_L=0.7 m	1739	3399	6876	13596	<0.01
Large, with d_L=1 m	1758	3438	6953	13752	<0.02

Results

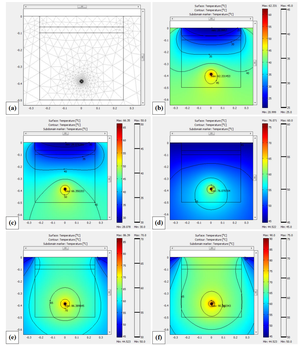

Figure 3. Temperature distribution over (a) the part of the computational domain from Fig. 2 that represents the cable trench, obtained for the case II when the upper surface of the trench is covered with (b) cool white coating, (c) acrylic white paint, (d) uncoated concrete blocks, (e) uncoated asphalt, and (f) acrylic black paint.

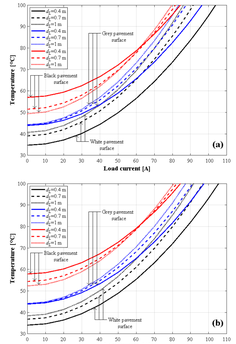

Figure 4. Temperature of the S-phase conductor versus load current for different laying depths and pavement surfaces: (a) bedding having dimensions 0.5 m × 0.4 m, and (b) trench completely filled with bedding material.

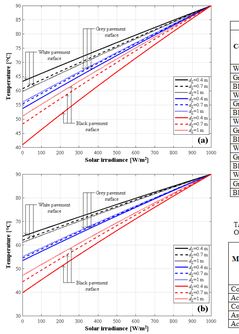

Figure 5. Temperature of the S-phase conductor versus solar irradiance for different laying depths and pavement surfaces: (a) bedding having dimensions 0.5 m × 0.4 m, and (b) trench completely filled with bedding material..

TABLE II. SIMULATION RESULTS OBTAINED FOR THE LABORATORY CONDITIONS

Pavement surface			Temperature						Q_s	I
Color	*Absorptivity, α*	*Emissivity, ε*	Phase conductors	Cable's outer surface		Pavement Lower surface		Upper surface		
				Sim.	*Diff.*	*Sim.*	*Diff.*	*Sim.*	*Diff.*	W/m	A
	–	–		°C	°C	°C	°C	°C	°C		
White	0.26	0.9	56.2	50	-1.4	25.12	-0.28	24.29	-0.11	242410	54.46
Grey	0.56	0.94	56.21	50	-1.3	25.11	+0.31	24.27	+0.57	242540	54.47
Black	0.97	0.91	56.2	50	-1.5	25.12	-1.38	24.28	-1.42	242440	54.46
White	0.26	0.9	62.35	55	-1.3	25.52	-0.38	24.52	-0.78	287310	59.29
Grey	0.56	0.94	62.36	55	-0.7	25.49	+1.39	24.5	+1.0	287450	59.3
Black	0.97	0.91	62.35	55	-1.4	25.51	-1.39	24.52	-1.48	287360	59.29
White	0.26	0.9	68.5	60	-1.1	25.91	+1.01	24.76	+1.26	332200	63.75
Grey	0.56	0.94	68.51	60	-0.6	25.88	+1.68	24.73	+1.23	332190	63.75
Black	0.97	0.91	68.5	60	-1.0	25.9	-1.0	24.75	-1.15	332250	63.76
White	0.26	0.9	74.65	65	-0.9	26.3	-0.6	25.0	-1.2	377100	67.92
Grey	0.56	0.94	74.66	65	-0.2	26.27	+1.47	24.97	+1.17	377110	67.94
Black	0.97	0.91	74.65	65	-0.8	26.29	-1.01	24.99	-1.31	377150	67.93
White	0.26	0.9	80.79	70	-0.9	26.69	-0.21	25.24	-0.66	421960	71.85
Grey	0.56	0.94	80.8	70	-0.3	26.66	+2.09	25.2	+1.6	422200	71.87
Black	0.97	0.91	80.8	70	-0.7	26.69	-0.41	25.23	-0.67	422070	71.86

"Sim." denotes the simulated value, while "Diff." denotes the difference between the simulated and experimental values.

TABLE III. EFFECT OF PAVEMENT SURFACE RADIATION PROPERTIES ON TEMPERATURES OF PAVEMENT, CABLE'S OUTER SURFACE AND S-PHASE CONDUCTOR FOR THE CASES I AND II RELATING TO THE LARGE-SIZE DOMAIN IN FIG. 2

Material, coating or paint	Surface radiation property		Case I Temperature			Case II Temperature		
	Absorptivity, α	*Emissivity, ε*	*Pavement surface*	*Cable's outer surface*	*S-phase conductor*	*Pavement surface*	*Cable's outer surface*	*S-phase conductor*
	–	–	°C	°C	°C	°C	°C	°C
Cool white coating	0.15	0.9	20.5	52.5	64.1	21	50.8	62.3
Acrylic white paint	0.26	0.9	27.7	56.3	67.9	28.1	54.9	66.4
Concrete blocks	0.56	0.94	45	65.5	77	45.2	64.7	76.1
Asphalt	0.87	0.93	63.3	75.3	86.6	63.2	75.1	86.4
Acrylic black paint	0.97	0.91	69.7	78.7	90	69.5	78.8	90

TABLE IV. VOLUME POWERS OF HEAT SOURCES AND CABLE AMPACITIES CALCULATED FOR THE LAYING DEPTH OF 0.7 METERS AND DIFFERENT THERMAL ENVIRONMENTS IN SUMMER AND WINTER

Material, coating or paint	Surface radiation property	Results obtained for the most unfavourable summer conditions				Results obtained for the most common winter conditions			
		Case I		*Case II*		*Case I*		*Case II*	
	α/ε	Q_s	I_{dc}	Q_s	I_{dc}	Q_s	I_{dc}	Q_s	I_{dc}
	–	W/m³	A	W/m³	A	W/m³	A	W/m³	A
Cool white coating	0.167	596590	85.4	682240	91.4	1018540	111.6	1122160	117.2
Acrylic white paint	0.289	572850	83.7	646280	88.9	1005330	110.9	1102250	116.1
Concrete blocks	0.596	515480	79.4	559140	82.7	973160	109.1	1051800	113.5
Asphalt	0.935	454920	74.6	466640	75.6	937180	107.1	999100	110.6
Acrylic black paint	1.066	433540	72.8	433950	72.9	924500	106.4	980110	109.5

Conclusions

- The simulated and experimental results are in good agreement.
- Compared to the corresponding cases with the black pavement, the ampacity of the considered cable laid at 0.7 m can be raised up to 25.6 % in summer and up to 10.2 % in winter.
- The ampacity of the considered cable was found to increase with decreasing the absorptivity-to-emissivity ratio of the pavement surface, as well as with decreasing the laying depth of the cable (excluding the case of black pavement surface for the range up to about 81 °C).
- All the ampacity values obtained for the laying depth of 0.7 m and the most unfavourable summer conditions are lower than the reference value of 111 A [11]. In addition, for the most common winter conditions, the ampacity values are lower or greater, by 4.6-6.2 amperes, than the reference value of 111 A.
- From the point of view of the solar irradiance, the ampacity of the considered cable increases with decreasing the laying depth in the case of grey or black pavement surface, and stays almost constant with decreasing the laying depth in the case of white pavement surface.
- The results obtained for the XLPE-cable changes according to a law similar to that observed in [4] for a PVC-cable.

Bibliography

1. International Electrotechnical Commission, IEC 60287-1-1:2006+AMD1:2014 CSV, Electric Cables – Calculation of the Current Rating – Part 1-1: Current Rating Equations (100% Load Factor) and Calculation of Losses – General, 2.1 edition, Geneva, Switzerland, 2014.
2. International Electrotechnical Commission, IEC TR 62095:2003, Electric cables – Calculations for current ratings – Finite element method, 1st edition, Geneva, Switzerland, 2003.
3. National Fire Protection Association, NFPA 70, National Electrical Code, 2017 Edition, Quincy, MA, USA, 2016.
4. D. Klimenta, B. Perović, J. Klimenta, M. Jevtić, M. Milovanović, I. Krstić, "Modelling the thermal effect of solar radiation on the ampacity of a low voltage underground cable," International Journal of Thermal Sciences, Vol. 134, 2018, pp. 507–516.
5. D. Klimenta, B. Perović, J. Klimenta, M. Jevtić, M. Milovanović, I. Krstić, "Controlling the thermal environment of underground cable lines using the pavement surface radiation properties," IET Generation, Transmission & Distribution, Vol. 12, Issue 12, 2018, pp. 2968–2976.
6. D. O. Klimenta, B. D. Perović, J. Lj. Klimenta, M. M. Jevtić, M. J. Milovanović, I. D. Krstić, "Controlling the thermal environment of underground power cables adjacent to heating pipeline using the pavement surface radiation properties," Thermal Science, Vol. 22, No. 6A, 2018, pp. 1–16.
7. L. Lindström, "Evaluating impact on ampacity according to IEC-60287 regarding thermally unfavourable placement of power cables," Masters' Degree Project, Royal Institute of Technology (KTH), Stockholm, Sweden, November 2011, XR-EE-ETK 2011:009.
8. J. Nahman, M. Tanaskovic, "Calculation of the ampacity of high voltage cables by accounting for radiation and solar heating effects using FEM," International Transactions on Electrical Energy Systems, Vol. 23, Issue 3, 2013, pp. 301–314.
9. J. Nahman, M. Tanaskovic, "Evaluation of the loading capacity of a pair of three-phase high voltage cable systems using the finite-element method," Electric Power Systems Research, Vol. 81, Issue 7, 2011, pp. 1550–1555.
10. J. Nahman, M. Tanaskovic, "Calculation of the loading capacity of high voltage cables laid in close proximity to heat pipelines using iterative finite-element method," International Journal of Electrical Power and Energy Systems, Vol. 103, 2018, pp. 310–316.
11. L. Heinhold, Power Cables and their Application – Part 1, third revised ed., Siemens Aktiengesellschaft, Berlin and Munich, Germany, 1990.

printed by MegaPrint Inc. www.postersession.com